Robust and low-cost interrogation technique for integrated photonic biochemical sensors based on Mach–Zehnder interferometers

V. Toccafondo[1,*] and C. J. Oton[2]

[1]*Consorzio Nazionale Interuniversitario per le Telecomunicazioni, Via G. Moruzzi 1, 56124 Pisa, Italy*
[2]*Scuola Superiore Sant'Anna, Via G. Moruzzi 1, 56124 Pisa, Italy*
**Corresponding author: veronica.toccafondo@cnit.it*

Received February 20, 2015; revised February 9, 2016; accepted February 16, 2016;
posted February 18, 2016 (Doc. ID 254169); published March 14, 2016

We describe and experimentally demonstrate a measuring technique for Mach–Zehnder interferometer (MZI) based integrated photonic biochemical sensors. Our technique is based on the direct measurement of phase changes between the arms of the MZI, achieved by signal modulation on one of the arms of the interferometer together with pseudoheterodyne detection, and it allows us to avoid the use of costly equipment such as tunable light sources or spectrum analyzers. The obtained output signal is intrinsically independent of wavelength, power variations, and global thermal variations, making it extremely robust and adequate for use in real conditions. Using a silicon-on-insulator MZI, we demonstrate the real-time monitoring of refractive index variations and achieve a detection limit of 4.1×10^{-6} refractive index units (RIU).

OCIS codes: (130.6010) Sensors; (130.3120) Integrated optics devices; (060.2840) Heterodyne.
http://dx.doi.org/10.1364/PRJ.4.000057

1. INTRODUCTION

Silicon photonics [1] is becoming a very attractive technology for the realization of photonic biosensors aimed at the detection of proteins, antibodies, DNA, contaminants, and so forth. The main reason for this is their potential for mass production because of being compatible with standard CMOS processes, which would yield a very low cost per device while maintaining a high sensing performance. However, at the moment they are hardly employed outside academic research and are struggling to find an appropriate market [2]. We believe that this is due to several factors, among which is the very conservative medical and biological environment, into which it is difficult to introduce disruptive technology, or the fact that many of those sensors rely on the use of expensive devices, such as tunable lasers or optical spectrum analyzers, to perform the readout of the sensor [2]. Moreover it is difficult to find integrated photonic biosensors which are really robust to environmental changes, such as the temperature of the surrounding medium or the power and wavelength fluctuations of the light source. Typically employed photonic structures include ring resonators [3], photonic crystals [4], microdisks [5], or Mach–Zehnder interferometers (MZIs) [6]. All these are based on evanescent wave sensing and exhibit a change in their response when the refractive index n_{eff} of the surrounding medium changes. The first three rely on the detection of a change in the transmission spectrum of the device when n_{eff} changes. In MZI-based sensors the phase difference induced by n_{eff} variations over one of the two interferometer arms yields a modulation of the interferometric conditions at the device output [2,6]. Typically this intensity variation is what is measured when using MZI-based sensors, but it presents some drawbacks, such as the change in sensitivity depending on the interferometric condition (maximum around the quadrature points, but very low at the vertices), and the intrinsic difficulty in distinguishing phase changes from intensity variations. A measuring technique allowing us to avoid this problem and in which the signal going through one of the MZI arms is electrically modulated was already proposed in [7], although the performance of the device with the modulation elements was not demonstrated. In that paper, the interrogation was based on a different technique in which a time delay between a trigger and the quadrature point was monitored. In [8] a technique was proposed for MZI interrogation based on phase modulation of the laser source. However, that technique requires a very asymmetric MZI which produces a phase response that is very sensitive to thermal fluctuations and wavelength variations of the source.

In this paper we propose a technique based on pseudoheterodyne phase demodulation [9], capable of extracting the phase variations in a robust way without having to tune the laser source or use spectral analysis. In our experiment we have used a dual-phase lock-in amplifier (LIA) for phase demodulation, although it is expected that simpler phase-demodulation components could be used too, which would avoid the need of lock-in amplification. Our technique is intrinsically immune to power, temperature, and wavelength fluctuations, and it allows the use of low-cost instruments to perform the read-out, making it very promising for the realization of low-cost point-of-care devices.

2. CONCEPT

The phase demodulation technique consists of the introduction of a periodic phase variation with a linear sawtooth with a 2π amplitude, which produces an effect equivalent to a

frequency shift, allowing heterodyne detection for the phase demodulation. The sinusoidal signal measured at the output has a phase difference with respect to the reference trigger which is equal to the optical phase difference between the two arms of the MZI. This technique was initially proposed for fiber-optic interferometers for applications in accelerometers and gyroscopes [9]. In this paper, we propose to use it in a photonic integrated circuit for detecting refractive index changes for the first time. In our experiment we have used a dual-phase LIA to measure the phase difference in real time, although simpler electronic phase demodulators are expected to work too, as the sinusoidal output had a good signal-to-noise ratio.

If the liquid that is on top of the sensitive waveguide is modified, the index difference produces the following phase difference at the output of the interferometer:

$$\Delta\varphi = \frac{2\pi}{\lambda} L \Delta n_{\text{eff}} = \frac{2\pi}{\lambda} L \frac{\partial n_{\text{eff}}}{\partial n_\ell} \Delta n_\ell, \tag{1}$$

where $\Delta\varphi$ is the measured phase difference, L is the length of the waveguide exposed to the liquid, λ is the laser wavelength, Δn_{eff} is the variation of the waveguide effective refractive index in the sensing arm, and n_ℓ the index of the liquid in the sensing arm.

3. FABRICATION

To demonstrate this technique, we have used a MZI fabricated in a silicon-on-insulator wafer with a 220 nm thick silicon layer on a 2 μm thick buried oxide layer. The fabrication of the structures was done through e-beam lithography at the Nanophotonics Technology Center of the Universidad Politecnica de Valencia, Spain. A 1.5 μm layer of SiO_2 was deposited as a top-cladding over the structure; then a window was opened over one of the MZI arms (the sensing arm) to allow the liquids under test to reach the waveguide surface and be detected. The other arm (reference arm) remained protected by the cladding. The total length of the exposed arm of the MZI was 10 mm, although it was wound in spirals occupying an area of 80 μm × 400 μm to make it compact. It was divided into four spirals to make each one fit in individual exposure frames. The length of the reference arm was almost the same as the sensing arm (just 1.63% longer to compensate for the group-index difference between the liquid-cladded and silica-cladded waveguide). The reason for this is to keep the MZI balanced, that is, with equal optical paths. This feature makes the interferometer immune to global temperature changes, as these equally affect both arms. In addition, it makes it immune to wavelength fluctuations of the laser source. In order to actively modulate the phase, a thermal modulator was introduced in the reference arm, which consisted in a spiraled 500 μm long narrow metal track on top of the waveguide and aligned with it, which was heated by the Joule effect applying a voltage up to 22 V.

450 nm wide single-mode waveguides are used in the sensing and reference arms and close to the Y-junction (used to split the input signal into the two MZI arms) and multimode interference coupler (used to recombine the signals after traveling through the interferometer), while the single-mode access waveguides are tapered to a width of 3 μm to reduce transmission losses far from bends and special elements. The whole device is accessed through TE-optimized grating couplers. An overview of the optical circuit is shown in Fig. 1(a), while a scanning electron microscope (SEM) micrograph of the sensing spirals is shown in Fig. 1(b).

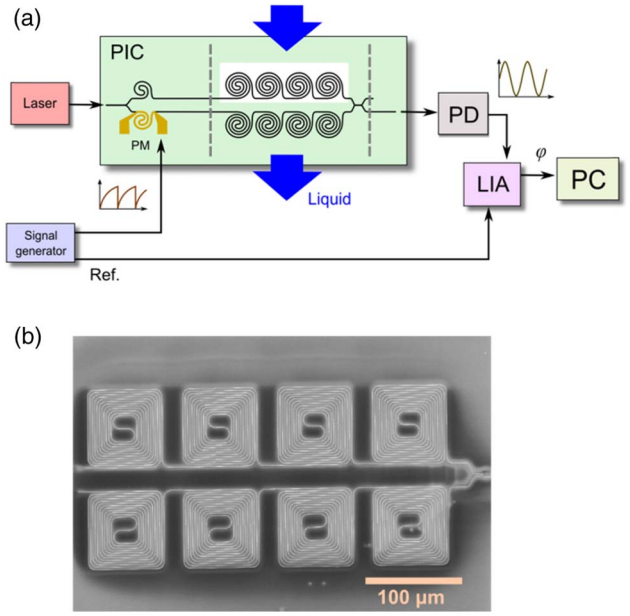

Fig. 1. (a) Setup used for the sensing experiments. The top spirals are exposed to the liquid (sensing arm), while the bottom ones are cladded and act as a reference. PIC, photonic integrated circuit; PM, phase modulator; PD, photodetector; PC, personal computer. (b) SEM micrograph of the spirals area.

Our chip was set on a micropositioner, and for the sensing experiments a polydimethylsiloxane (PDMS) cell with two outlets was clamped on top of it. Teflon tubing was used to connect the PDMS cell to a syringe on one side and to the vials containing the liquids under test on the other side. The syringe was used to manually pull the different liquids from the vials to the sample. The total size of the device was about 8000 μm × 180 μm, although most of the space was related to the margins needed by the fluidic channel.

4. EXPERIMENT AND RESULTS

The setup for the sensing experiment is shown in Fig. 1(a). The total fiber-to-fiber loss of the device was high (about 50 dB), while the coupling loss was 6 dB per grating from a reference sample. The high total loss is probably due to stitching effects associated with multiframe e-beam lithography, and for that reason we had to amplify the input laser (Photonetics Tunics) with an erbium-doped fiber amplifier (EDFA), yielding an input power in fiber of 20 dBm. However, using standard UV lithography for silicon photonics, assuming typical loss values of ~3 dB/cm and grating efficiency of ~4 dB, we would have a total loss of less than 12 dB, meaning that amplification would not be necessary. Considering that the MZI is balanced, a narrow laser linewidth is unnecessary in this setup; therefore lower cost distributed-feedback lasers would be suitable for this measurement. The wavelength of the laser was set to 1560 nm.

Additionally, the setup included a programmable signal generator, which was set to generate a square-root shape from zero to 22 V, which corresponded to a 2π phase shift. The

signal was sent to the integrated thermal phase modulator, which generated a linear sawtooth in phase, as the phase shift is proportional to the square of the voltage. The frequency was 80 Hz, which is orders of magnitude lower than the response times of this kind of modulators, which is in the order of microseconds [10]. If faster modulation speeds were needed, one could make use of integrated modulators, which are several orders of magnitude faster [11].

The sinusoidal output was measured with an amplified InGaAs photodiode and sent to the dual-phase LIA model SR-830 for phase demodulation. It is expected that for a photonic circuit with lower loss, lock-in amplification would not be necessary, but a simple solution like an analog phase demodulator electronic component would perform the phase extraction. Finally, the unwrapping of the phase profile was performed in real time via software, by detecting phase discontinuities higher than π and counting them to track the number of cycles. This procedure allowed us to track phase variations higher than one cycle.

The first sensing experiment was carried out using isopropyl alcohol (IPA) in water dilutions. We used 0.5%, 1%, and 2% IPA in water (the fraction of IPA is given in volume). We typically introduced water at time $t = 0$ s, then switched to an IPA concentration, alternating with water between different concentrations.

The phase variation we measured using the setup described before is reported in Fig. 2, where we can clearly see an instantaneous phase shift when the IPA–water solution reaches the sensor. We switched between the different concentrations and pure water several times to check for reproducibility.

The second experiment shows the phase response of the system for different concentrations of glycerol in water (here too the concentration is given in volume). In this experiment, the EDFA was not used and an input power of 5 dBm (in input fiber) was used. Results are shown in Fig. 3.

We also extracted the quantitative values of the observed shifts for several repetitions and different concentrations, and the results for both liquids are shown in Fig. 4. A linear response was observed in both cases.

In order to calculate the sensitivity of our sensor, we determined the refractive index of the solutions. Data for the refractive index of IPA in deionized water (DIW) solutions at 25°C was extracted from [12]. The data provided are in the visible range; however, data for water (0% IPA) and for 100% IPA in the infrared, at the same temperature, were taken from [13].

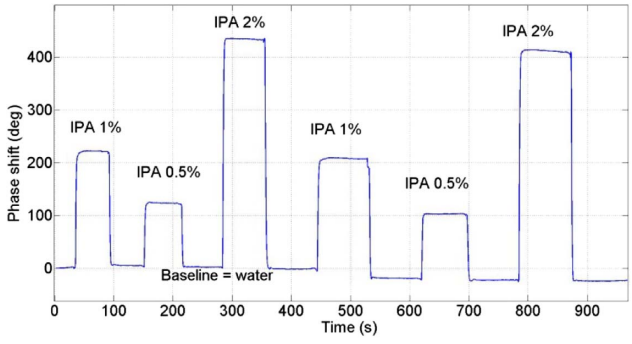

Fig. 2. Real-time refractive index sensing for IPA-in-water solutions. Phase shift versus time is reported for different IPA-in-water concentrations.

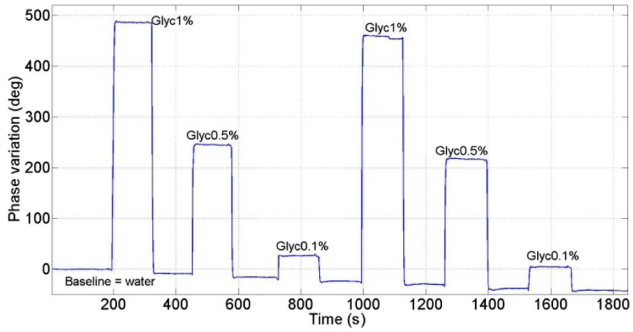

Fig. 3. Phase shift versus time for different glycerol concentrations in water.

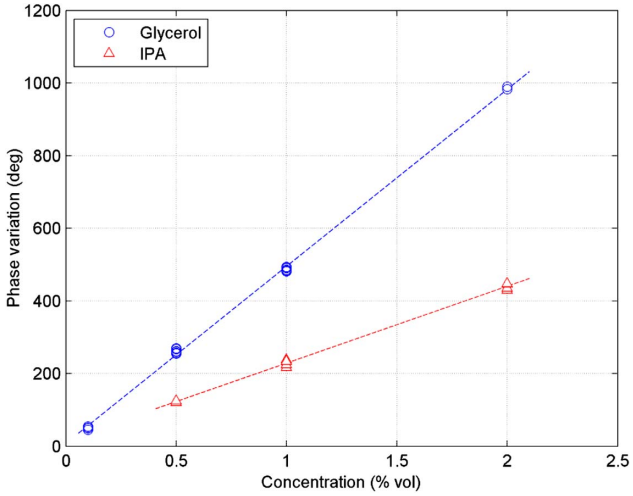

Fig. 4. Measured response for different concentrations of glycerol (circles) and IPA (triangles). Linear fits of the response versus concentration for each case are also shown.

Noting that the refractive index of the solution is not linear with its concentration, we took the trend in the visible range and extrapolated it to the infrared values, extracting the whole curve. Within small concentrations, the dependence is linear.

Data for the refractive index of glycerol in DIW solutions at 25°C was taken from [14]. Since we did not have data in the infrared region, we assumed the index difference between water and glycerin to be the same in the visible and infrared.

Table 1 shows the refractive indices of small concentrations of IPA and glycerol, together with the calculation of the variation of effective refractive index in the waveguide expected from the introduction of 2% of substance. This

Table 1. Refractive Index Values (at 1.55 μm) of IPA and Glycerol Aqueous Solutions at Low Concentrations, Together with Effective Index Variation Calculations and Expected Phase Response Extracted from Eq. (1)

	IPA	Glycerol
n (0%)	1.31500	1.31500
n (2%)	1.31681	1.3177
Δn (0–2%)	1.81×10^{-3}	2.70×10^{-3}
Δn_{eff} (0–2%)	3.69×10^{-4}	5.51×10^{-4}
Expected $\Delta\varphi$ (0-2%) (deg)	858	1279

calculation was performed using a finite difference eigenmode solver (MODE Solutions from Lumerical). With our waveguide geometry and TE polarization, a given liquid index change produces a change of 20.4% in the effective refractive index, which is the index directly measured in our interferometer.

With these estimations, we applied Eq. (1) to calculate the expected phase variation for the introduction of 2% of IPA or glycerol; the results are shown in Table 1, where 858° and 1279° were obtained, respectively. We can compare these values with the experimental responses we measured (shown in Fig. 4), which were 440° and 982°, respectively. One reason for the discrepancy is that we used the nominal parameters of the geometry of the waveguides, which may be slightly different due to fabrication errors. On the other hand, the vials in which we put the solutions were open during part of the experiment, so part of the solute might have evaporated during the experiments, especially for the IPA, which is very volatile. This would mean a slight decrease in its concentration, with a consequent decrease in the measured refractive index variation.

Equation (1) was also applied to calculate the experimental sensitivity S of the refractive index sensor, which we define as the phase shift per RIU of the liquid; for the fabricated sensor, which has an interaction length of 10 mm, we obtain $S = \Delta\phi/\Delta n_\ell = 3.64 \times 10^5$ deg /RIU equal to 6348 rad/RIU for the glycerol sensing experiment. However, the sensitivity itself could easily be increased by simply prolonging the interaction length (as the waveguides are spirally shaped, the resulting device would still be very compact). Another way of increasing the sensitivity would be a modification of the waveguide geometry or polarization, in order to increase the fraction of light that propagates through the liquid, like in [6], where they achieved a sensitivity of 1885 rad/RIU in a 1.5 mm long interferometer.

Concerning the detection limit (DL), which is defined as the smallest detectable index change, we calculated it using the following equation:

$$\mathrm{DL} = \frac{3\sigma}{S}, \tag{2}$$

where σ is the noise level. In our case, we calculated the noise level as the standard deviation of the signal in different regions where there were no variations in the liquid concentration. The obtained average value was $\sigma = 0.5°$; we thus calculate a $\mathrm{DL} = 4.1 \times 10^{-6}$ RIU. Considering that we performed our measurements with manual operation of the liquids, we are confident that we could achieve a lower noise level, and thus lower DL, in an automated setup. In addition, the optical loss of the system was very high, which also introduced noise in the phase demodulation process. Figures 2 and 3 also show a weak baseline drift of the order of tens of degrees in about 15 min, most likely related to the lack of thermal control of the liquids and the substrate. However, we stress that the key point of this paper is not the sensitivity of the sensor or its stability in this particular setup configuration, but the proof-of-principle for an active phase interrogation technique for the interferometer, which can dramatically reduce the cost of the sensor system.

5. CONCLUSIONS

We have demonstrated a technique for the active interrogation of integrated photonic biochemical sensors. Experiments show that we can achieve real-time phase demodulation with good sensitivity and low DLs, while using a robust and low-cost technique, making it suitable for the realization of inexpensive, portable, point-of-care devices. Future experiments will include sensing of biochemical binding events on the chip, through the functionalization of their surface and use of typical assays, such as, but not limited to, antibody–antigen. This demodulation technique could also be applied to other types of integrated interferometric sensors [15,16].

REFERENCES

1. H. Subbaraman, X. Xu, A. Hosseini, X. Zhang, Y. Zhang, D. Kwong, and R. T. Chen, "Recent advances in silicon-based passive and active optical interconnects," Opt. Express **23**, 2487–2511 (2015).
2. M. C. Estevez, M. Alvarez, and L. M. Lechuga, "Integrated optical devices for lab-on-a-chip biosensing applications," Laser Photon. Rev. **6**, 463–487 (2012).
3. T. Claes, J. G. Molera, K. De Vos, E. Schacht, R. Baets, and P. Bienstman, "Label-free biosensing with a slot-waveguide-based ring resonator in silicon on insulator," IEEE Photon. J. **1**, 197–204 (2009).
4. J. García-Rupérez, V. Toccafondo, M. J. Bañuls, J. García Castelló, A. Griol, S. Peransi-Llopis, and Á. Maquieira, "Label-free antibody detection using band edge fringes in SOI planar photonic crystal waveguides in the slow-light regime," Opt. Express **18**, 24276–24286 (2010).
5. M. S. Luchansky and R. C. Bailey, "High-Q optical sensors for chemical and biological analysis," Anal. Chem. **84**, 793–821 (2012).
6. A. Densmore, D. X. Xu, P. Waldron, S. Janz, P. Cheben, J. Lapointe, A. Delâge, B. Lamontagne, J. H. Schmid, and E. Post, "A silicon-on-insulator photonic wire based evanescent field sensor," IEEE Photon. Technol. Lett. **18**, 2520–2522 (2006).
7. R. G. Heideman and P. V. Lambeck, "Remote opto-chemical sensing with extreme sensitivity: design, fabrication and performance of a pigtailed integrated optical phase-modulated Mach–Zehnder interferometer system," Sens. Actuators B Chem. **61**, 100–127 (1999).
8. S. Dante, D. Duval, B. Sepúlveda, A. B. González-Guerrero, J. R. Sendra, and L. M. Lechuga, "All-optical phase modulation for integrated interferometric biosensors," Opt. Express **20**, 7195–7205 (2012).
9. D. A. Jackson, A. D. Kersey, M. Corke, and J. D. C. Jones, "Pseudoheterodyne detection scheme for optical interferometers," Electron. Lett. **18**, 1081–1083 (1982).
10. A. Masood, M. Pantouvaki, G. Lepage, P. Verheyen, J. Van Campenhout, P. Absil, D. Van Thourhout, and W. Bogaerts, "Comparison of heater architectures for thermal control of silicon photonic circuits," in *IEEE 10th International Conference on Group IV Photonics (GFP)* (2013), pp. 83–84.
11. G. T. Reed, G. Mashanovich, F. Y. Gardes, and D. J. Thomson, "Silicon optical modulators," Nat. Photonics **4**, 518–526 (2010).
12. K. Y. Chu and A. R. Ralph Thompson, "Densities and refractive indices of alcohol-water solutions of n-propyl, isopropyl, and methyl alcohols," J. Chem. Eng. Data **7**, 358–360 (1962).
13. C. B. Kim and C. B. Su, "Measurement of the refractive index of liquids at 1.3 and 1.5 micron using a fibre optic Fresnel ratio meter," Meas. Sci. Technol. **15**, 1683–1686 (2004).
14. F. Koohyar, A. A. Rostami, M. J. Chaichi, and F. Kiani, "Study on thermodynamic properties for binary systems of water+L-cysteine hydrochloride monohydrate, glycerol, and d-sorbitol at various temperatures," J. Chem. **2013**, 601751 (2013).
15. J. T. Robinson, L. Chen, and M. Lipson, "On-chip gas detection in silicon optical microcavities," Opt. Express **16**, 4296–4301 (2008).
16. G. D. Kim, H. S. Lee, C. H. Park, S. S. Lee, B. T. Lim, H. K. Bae, and W. G. Lee, "Silicon photonic temperature sensor employing a ring resonator manufactured using a standard CMOS process," Opt. Express **18**, 22215–22221 (2010).